A NEW QUASI Z-SOURCE EMBEDDED NETWORK CAPABLE OF PRODUCING DC-SIDE VOLTAGE GAIN EVEN WITHOUT SHOOT-THROUGH STATE FOR EFFICIENT OPERATION

Pritam Kumar Gayen*

Department of Electrical Engineering, Kalyani Government Engineering College, Kalyani, West Bengal, India

ARTICLE INFO

***Article history*:**
Received: 27.03.2024.
Received in revised form: 05.06.2024.
Accepted: 25.07.2024.

Keywords:
Versatile Quasi Z-source Inverter
Non-shoot-through Duty Ratio-based Voltage Gain
Fixed Modulation Index Operation
Control Flexibility
Efficiency

DOI: https://doi.org/10.30765/er.2489

Abstract:

The conventional quasi-z-source inverter (QZSI) is not capable of producing DC-side voltage gain without shoot-through operation. This restricts freedom of control and performance. The decoupled control between modulation index (MI) and duty ratio for producing DC-side voltage gain at MI = 1 is not permitted. In this context, this paper proposes a novel active-switched impedance network. This is capable of producing DC-side voltage gain either in shoot-through mode or in the absence of shoot-through state. In effect, variable DC-side voltage gains are achieved at a fixed value of MI, even at MI = 1 (without the dead-time requirement of the inverter bridge). For low-gain operations (up to 2.5), the DC-side voltage gain is achieved by the proposed active-switched QZSI by restricting the shoot-through duty ratio to a low value (0-0.1). In high-gain (>2.5) operations, the variable-boosting operations of the proposed QZSI are achieved without shoot-through operation (MI = 1) by controlling its active switch. This increases efficiency by discarding the shoot-through state at high gain. The suggested closed-loop control logic of the proposed QZSI is also provided to meet the load voltage. The simulation work is conducted in versatile operating conditions to highlight its diversified performances. The experiments also verify its operations under different conditions.

1 Introduction

There are various types of quasi-z-source inverters (QZSI) [1, 2] that have been proposed by the researchers for practical usage after the inception of ZSI [3]. The topology is mainly used in converting low DC voltage directly into AC voltage in the applications of solar power conversion systems and electrical vehicles. This is a single-stage power inverter with several advantages over a two-stage power conversion that consists of a cascaded connection of a boost converter and a voltage source inverter. The advantages are cited as both bucking and boosting of voltage conversion, pulse width modulation (PWM) of the power switch of the inverter bridge without dead time in the switching signal, reliable operation by sustaining shoot-through operation of the power switches, and no dead time-prone distortion or electromagnetic interference. The impedance network of QZSI provides DC-side voltage gain along with the prevention of short-circuit current at the DC source or DC bus. The non-isolated topologies for the last two decades are developed, namely extended boost [4], enhanced boost [5], high boost or gain [6, 7], ultra-high gain [8], enhanced ultra-high gain [9], etc. All works emphasize the improvement of shoot-through-based voltage gain by reducing the range of the shoot-through duty ratio. This accomplishes the operation of QZSI with a high value of modulation index (MI). There is a coupling [10] between the relationship between shoot-through duty ratio and MI. The decoupling between the two control variables is not permissible in the above-mentioned topologies. The shoot-through state, zero state, and active state of PWM signals [11-13] are required to be chosen such that the

* Corresponding author
E-mail address: pkgtar@gmail.com

required DC-side voltage-boosting action and power requirement at the AC-side are simultaneously fulfilled. The shoot-through state decides the voltage boost, whereas the MI decides the amplitude of the AC voltage. Here, the restriction of shoot-through span in PWM signals at high MI puts a limit on the voltage boost. Thus, high gain at a high modulation index cannot be achieved. On the contrary, the MI is lowered at higher voltage gain. This increases total harmonic distortion (THD). Thus, the QZSI (Figure 1(a)) lacks control freedom. In [14-16], different topologies with control freedom are suggested. Here, shoot-through-less variable voltage-boosting actions are not noticed, thus control flexibility is partially restricted. The comparisons with the features stated in the state-of-arts are given in Table 1.

Table 1. Comparative features among state-of-arts.

Network in Reference	No. of Active Switch	Shoot-through - based Gain	Shoot-through-less Gain	Variable Boosting at M=1	Dead Time
[5]	1	$\frac{1}{1-4D_{sh}+2D_{sh}^2}$	No	No	No
[6]	1	$\frac{1}{1-4D_{sh}+2D_{sh}^2}$	No	No	No
[7]	1	$\frac{2}{1-4D_{sh}+2D_{sh}^2}$	No	No	No
[14]	1	$\frac{1}{1-2D_{sh}}$	No	No	No
[15]	2	$\frac{1-ND_{sh}}{1-(2+N)D_{sh}}$	No	No	No
[16]	2	$\frac{1+D_1}{1-2D_{sh}}$	No	No	Yes
Proposed	1	$\frac{2}{1-2D_{sh}}$	Yes- $\frac{1}{1-D_{s7}}$	Yes	No

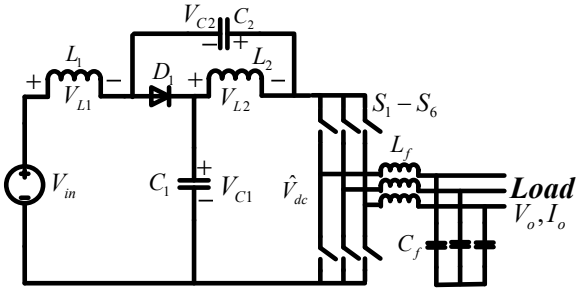

(a) Conventional QZSI

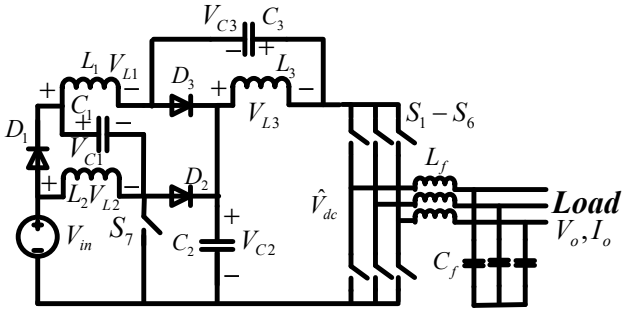

(b) Proposed QZS network-based inverter

Figure 1. Conventional and proposed QZSIs.

In this context, a versatile active-switched QZSI is proposed, which primarily facilitates the flexibility of controlling DC-side voltage gain irrespective of the value of MI and also enhances shoot-through-based voltage gain. Here, the separate duty ratio control provides variable *shoot-through-less* gains to further enhance control flexibility.
The following distinguishable features of the suggested impedance network are mentioned:

i. The suggested QZSI provides DC-side voltage gain without shoot-through operation. This feature is not noticed for existing QZSIs in the literatures,
ii. The duty ratio of the active switch (S7 in Figure 1(b)) is different from the shoot-through duty ratio of inverter bridge switches, unlike many conventional QZSIs,
iii. The ON time of the active switch (S_7 in Figure 1(b)) of the proposed impedance network is permitted to extend during the non-shoot-through period for flexibility of control,
iv. The adjustment of DC-side voltage gain can be decoupled from the adjustment of modulation index (or shoot-through duty ratio).
v. The shoot-through duty ratio-based DC-side voltage gain is also increased through the proposed active switched QZSI,
vi. A high boost in voltage is possible with joint controls of the duty ratios during shoot-through and non-shoot-through operations,
vii. The low shoot-through or non-shoot-through-based boosting action improves efficiency.

The operation of the suggested inverter along with its modulation method are discussed in section 2. Different mathematical analyses to characterize the performance of the proposed QZSI are also provided in section 3. The investigations and results of different studies are described in section 4. Section 5 concludes the findings.

2 Operation of proposed quasi-Z-source inverter

The conventional and proposed QZSIs are shown in Figure 1. The suggested active switched impedance network (Figure 1(b)) comprises inductors (L_1, L_2, L_3), capacitors (C_1, C_2, C_3), diodes (D_1, D_2, D_3), and an independently controlled switch (S_7). Here, different power switches are controlled as follows:

(i) Shoot-through duty ratio adjustments are made through the control of power switches in the inverter bridge,

(ii) The duty ratio of switch 'S7' is separately controlled from the inverter bridge switches. Thus, duty ratio control during the non-shoot-through stage is permitted. In effect, variable DC-side voltage gains are obtained irrespective of the MI of the inverter bridge.

Sometime, the anti-parallel switch [17] across D_1 (Fig. 1(a)) or D_3 (Figure 1(b)) avoids the irregularities in DC-bus voltage [18] for the wide power range of operation [19] of the power converters in Fig. 1. This also helps to improve the voltage gain of proposed QZSI in Figure 1(b).

2.1 Shoot-through (ST) state (0-T_{st})

In this state- S_1- S_7: ON; D_2 and D_3: OFF; D_1: ON; L_1, L_2 and L_3: Charging; C_1: Charging and C_2, C_3: Discharging.

2.2 Non-shoot-through (NST) state (T_{sh} -T_{s7} and T_{s7} -T_o)

In this state- S_1- S_7: ON; D_2 and D_3: OFF; D_1: ON; L_1, L_2 and L_3: Charging; C_1: Charging and C_2, C_3: Discharging.

The operation in either sub-mode 2a (Figure 2(c)) or sub-mode 2b (Figure 2(d)) occurs on the basis of either non-conduction ($D_{s7}\leq 0.5$) or conduction ($D_{s7}>0.5$) of diode 'D_2', respectively.

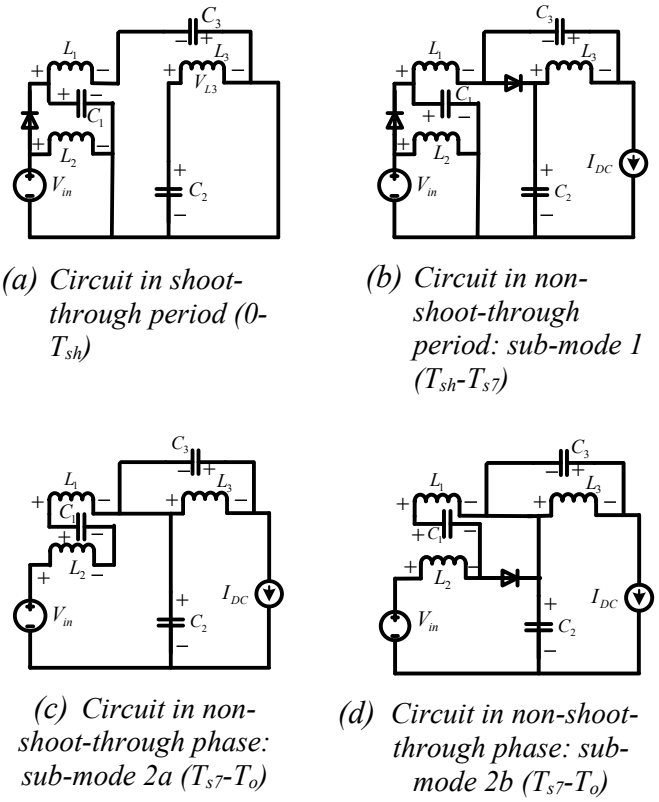

(a) Circuit in shoot-through period (0-T_{sh})

(b) Circuit in non-shoot-through period: sub-mode 1 (T_{sh}-T_{s7})

(c) Circuit in non-shoot-through phase: sub-mode 2a (T_{s7}-T_o)

(d) Circuit in non-shoot-through phase: sub-mode 2b (T_{s7}-T_o)

Figure 2. Circuits during different operations.

2.3 Pulse width modulation (PWM) logic

The simple boost control (SBC) PWM [3] technique for the proposed QZSI is applied. The PWM signals for the upper switches of the inverter bridge, shoot-through pulse, and pulse for switching of 'S_7' are shown in Figure 3. Here, the various duty cycles of the PWM signals are taken as D_{sh}=0.25 (M=0.75), and D_{s7}=0.6 for the illustration.

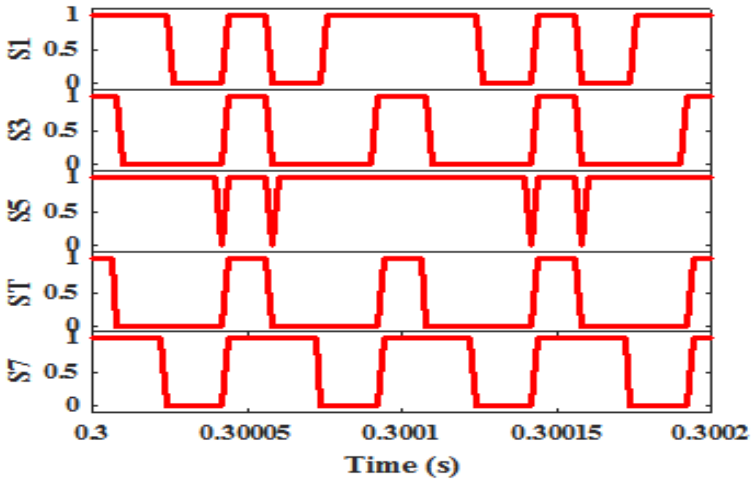

Figure 3. Pulses for switching of upper leg switches and S7, and ST state.

3 Performance and control of proposed quasi-Z-source inverter

The various issues are discussed as follows:

3.1 Various stresses on different elements

In the suggested QZSI (Figure 1(b)), two types of DC-side voltage gain arise in consideration of the circuits in Figures 2(c) and 2(d), depending on the gain range. These are presented as follows:

3.1.1 Voltage gain (≤2.5) from the modes in Figures. 2(a) and 2(c)

The Volt-Sec equations for the inductors 'L_1 and L_2' together in switching period (T_s) are mathematically written:

$$\int_0^{T_s} \left(V_{L1} + V_{L2}\right) dt = 0 \tag{1}$$

The equation in (2) is expressed from (1) as,

$$\begin{aligned} &\left(V_{in} + V_{C3}\right) D_{sh} + \left(V_{in} - V_{C2}\right)\left(D_{s7} - D_{sh}\right) + V_{in} D_{s7} \\ &+ \left(V_{in} + V_{C1} - V_{C2}\right)\left(1 - D_{s7}\right) = 0 \end{aligned} \tag{2}$$

Here, the shoot-through duty ratio and duty ratio of active switch (S_7) are symbolized as 'D_{sh}' and 'D_{s7}', respectively.

In case of the inductor 'L_3' as,

$$D_{sh} V_{C2} + \left(1 - D_{sh}\right)\left(-V_{C3}\right) = 0 \tag{3}$$

From (3), it is given in below,

$$V_{C3} = \left(\frac{D_{sh}}{1 - D_{sh}}\right) V_{C2} \tag{4}$$

From (2) and (4), the capacitor is derived as given below,

$$V_{C2} = \begin{cases} \dfrac{\left(1 + D_{s7}\right)\left(1 - D_{sh}\right)}{\left(1 - 2D_{sh}\right)} V_{in} \\ + \dfrac{\left(1 - D_{s7}\right)\left(1 - D_{sh}\right)}{\left(1 - 2D_{sh}\right)} V_{C1} \end{cases} ; V_{C1} = V_{in} \tag{5}$$

The peak value of DC-bus voltage is calculated from (6) using (4) and (5),

$$\hat{V}_{dc} = V_{C2} + V_{C3} = B_{p1}.V_{in} = 2.V_{in} / \left(1 - 2D_{sh}\right) \tag{6}$$

In (6), boosting factor is denoted as 'B_{p1}'. The gain of conventional QZSI is,

$$B_c = \frac{1}{1 - 2D_{sh}} \tag{7}$$

The plots in Figure 4 present the enhancement of shoot-through-based voltage gain is achieved for the proposed case in comparison to conventional gain up to gain value of 2.5.

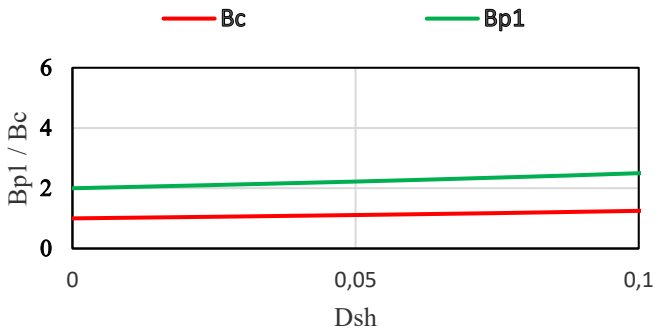

Figure 4. B_{p1} vs. D_{sh} using (6).

3.1.2. Voltage gain (>2.5) from the modes in Figures. 2(a), 2(b) and 2(d)

In the inductor 'L_2', the mathematical expression is written,

$$D_{s7}V_{in} + (1 - D_{s7})(V_{in} - V_{C2}) = 0 \tag{8}$$

From (4) and (8), the following equations are derived,

$$V_{C2} = \left(\frac{1}{1 - D_{s7}}\right).V_{in}; \quad V_{C3} = \left(\frac{D_{sh}}{1 - D_{sh}}\right)\left(\frac{1}{1 - D_{s7}}\right).V_{in} \tag{9}$$

Therefore, the peak of DC-bus voltage is,

$$\hat{V}_{dc} = \left(\frac{1}{1 - D_{sh}}\right)\left(\frac{1}{1 - D_{s7}}\right).V_{in} = B_p.V_{in} \tag{10}$$

In (10), the 'B_p' indicates boosting gain. Its value is finite even at 'D_{sh}=0'. In (4)-(6) and (10), the duty ratios and MI varies as, $0<D_{sh}<0.5$, $0<D_{s7}<1$ and $0<M\leq 1$.
The plots in Figure 5 reveal that the boosting gain is varying with the variations of the duty ratio (D_{s7}) of the active switch 'S_7'. Here, the gain due to the variation increases at a particular value of shoot-through duty ration (D_{sh}). Thus, it indicates decoupled duty ratio control of 'S_7' from shoot-through duty ratio is permissible using the proposed QZSI to obtain variable DC-side voltage gains even at 'D_{sh}=0'.

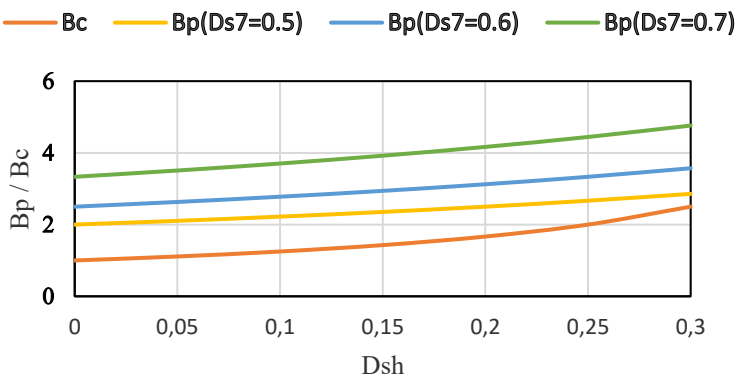

Figure 5. B vs. D_{sh} under variable D_{s7} using (10).

3.2 Proposed closed loop voltage control

The proposed closed loop control logic for regulating its output voltage is shown in Figure 6. Here, the boosting gain value up to 2.5 (threshold value) is considered as low-gain, and the output voltage is controlled by 'D_{sh}=D_{s7}' (range: 0-0.1). For high-gain operation, the output voltage is regulated by adjusting 'D_{s7}' (0.5-0.75) only at fixed M=1 (D_{sh}=0) as given in Figure 6.

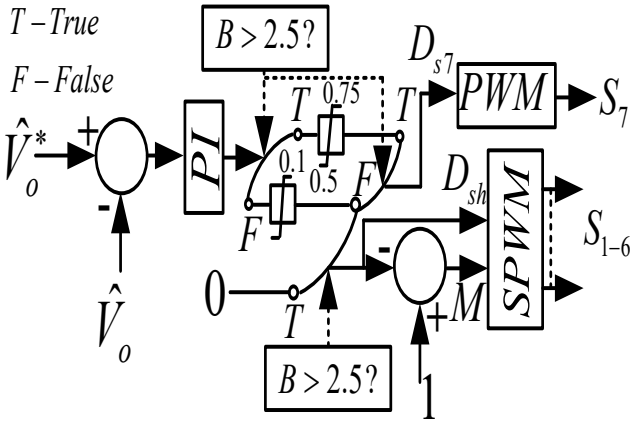

Figure 6. Proposed control logic diagram.

3.3 Power losses

The derived current expressions for calculating losses in different elements of the proposed inverter are listed in Table 2. The efficiency at varying gains is shown in Figure 7, which shows improved efficiency in the case of proposed control in Figure 6.

Table 2. Current and Loss expressions.

Element	Current	Loss
L:	$B \le 2.5: \begin{cases} I_{L1(RMS)} = I_{L2(RMS)} = \dfrac{1-D_{sh}}{1-3D_{sh}+D_{sh}^{2}} I_{DC} \\ I_{L3(RMS)} = \dfrac{1}{1-3D_{sh}+D_{sh}^{2}} I_{DC} \end{cases}$; $B > 2.5: \begin{cases} I_{L1(RMS)} = 0 \\ I_{L2(RMS)} = \dfrac{1}{1-D_{s7}} I_{DC} \\ I_{L3(RMS)} = I_{DC} \end{cases}$	$P_L = I_{L1(RMS)}^2 r_{L1} + I_{L2(RMS)}^2 r_{L2} + I_{L3(RMS)}^2 r_{L3}$
C:	$B \le 2.5: \begin{cases} I_{C1(RMS)} = \dfrac{(1-D_{sh})^{3/2}\sqrt{1/D_{sh}}}{1-3D_{sh}+D_{sh}^{2}} I_{DC} \\ I_{C2(RMS)} = \dfrac{\sqrt{D_{sh}/1-D_{sh}}}{1-3D_{sh}+D_{sh}^{2}} I_{DC} \\ I_{C3(RMS)} = \dfrac{\sqrt{D_{sh}(1-D_{sh})}}{1-3D_{sh}+D_{sh}^{2}} I_{DC} \end{cases}$; $B > 2.5: \begin{cases} I_{C1(RMS)} = 0 \\ I_{C2(RMS)} = \sqrt{D_{s7}/1-D_{s7}}.I_{DC} \\ I_{C3(RMS)} = 0 \end{cases}$	$P_C = I_{C1(RMS)}^2 r_{C1} + I_{C2(RMS)}^2 r_{C2} + I_{C3(RMS)}^2 r_{C3}$
D:	$B \le 2.5: \begin{cases} I_{D1(AVG)} = \dfrac{(1-D_{sh})}{1-3D_{sh}+D_{sh}^{2}} I_{DC}; I_{D1(RMS)} = \dfrac{(1-D_{sh})}{\sqrt{D_{sh}}(1-3D_{sh}+D_{sh}^{2})} I_{DC} \\ I_{D2(AVG)} = 0; I_{D2(RMS)} = 0 \\ I_{D3(AVG)} = \dfrac{(1-D_{sh})}{1-3D_{sh}+D_{sh}^{2}} I_{DC}; I_{D3(RMS)} = \dfrac{1}{\sqrt{1-D_{sh}}(1-3D_{sh}+D_{sh}^{2})} I_{DC} \end{cases}$ $B > 2.5: \begin{cases} I_{D1(AVG)} = 0; I_{D1(RMS)} = 0 \\ I_{D2(AVG)} = 0; I_{D2(RMS)} = 0 \\ I_{D3(AVG)} = I_{DC}; I_{D3(RMS)} = \dfrac{I_{DC}}{\sqrt{1-D_{s7}}} \end{cases}$	$\begin{cases} P_{rr} = 3Q_{rr}F_s\hat{V}_{dc}; \\ P_{fd} = \left(I_{D1(AVG)} + I_{D2(AVG)} + I_{D3(AVG)}\right).V_F; \\ P_{oh} = \left(I_{D1(RMS)}^2 + I_{D2(RMS)}^2 + I_{D3(RMS)}^2\right).r_D \\ P_D = P_{rr} + P_{fd} + P_{oh} \end{cases}$
S_7:	$B \le 2.5: \begin{cases} I_{S7(AVG)} = \dfrac{2D_{sh}(1-D_{sh})}{1-3D+D^2} I_{DC} \\ I_{S7(RMS)} = \dfrac{2\sqrt{D_{sh}}(1-D_{sh})}{1-3D+D^2} I_{DC} \end{cases}$; $B > 2.5: \begin{cases} I_{S7(AVG)} = \dfrac{D_{s7}}{1-D_{s7}} I_{DC} \\ I_{S7(RMS)} = \dfrac{\sqrt{D_{s7}}}{1-D_{s7}} I_{DC} \end{cases}$	$\begin{cases} P_{SW7} = \dfrac{(T_{on}+T_{off})}{2}.F_S.V_{S7}.I_{S7(AVG)} \\ P_{COND7} = I_{S7(RMS)}^2.r_{S7} \end{cases}$ $P_{sw7} = P_{SW7} + P_{COND7}$
$S_{1\text{-}6}$:	$I_{S\_inv(RMS)} = \sqrt{\dfrac{D}{9}.I_{sh}^2 + \dfrac{16(1-D)P_o^2}{9\pi^2 M^2 B^2 V_{DC}^2.\cos^2\phi}}$ $I_{Sh} = I_{L1} + I_{L3}$	$\begin{cases} P_{SW(INV)} = 6.\dfrac{(T_{ON}+T_{OFF})}{2}.F_S.\hat{V}_{DC}.\dfrac{I_{sh}}{3} \\ P_{COND(INV)} = 6.I_{S\_inv(RMS)}^2.r_{S\_inv} \end{cases}$ $P_{sw} = P_{SW(INV)} + P_{COND(INV)}$

Efficiency: $\eta = \dfrac{V_{in}I_{L1} - \left(P_L + P_C + P_D + P_{sw} + P_{sw7}\right)}{V_{in}I_{L1}}$

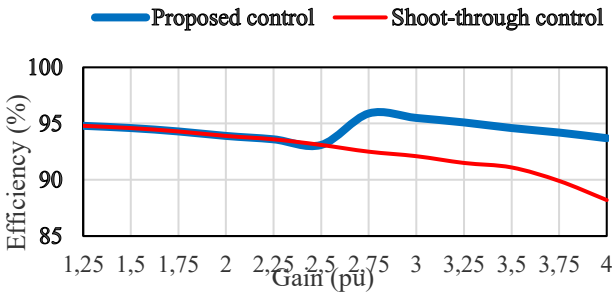

Figure 7. Efficiency.

3.4 *Operation without shoot-through state (M=1)*

The circuit diagram for the special operation of the proposed inverter at M=1 is shown in Figure 8. The shoot-through-less DC-voltage boosting operation is possible due to the circuit configuration in this operation. This does not require dead time for the inverter bridge switches due to the presence of 'L_3'.

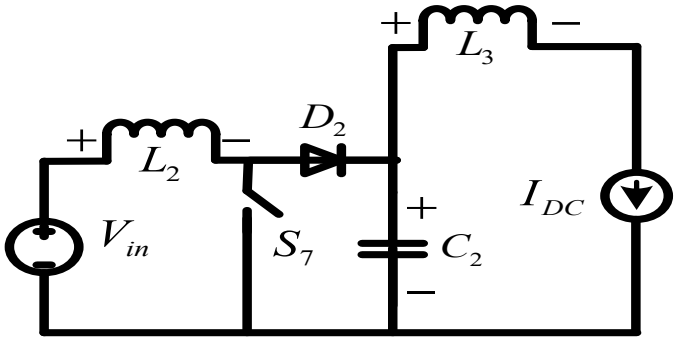

Figure 8. Circuit under the operation at M=1 (D_{sh}=0).

4 Studies and results

The simulation and experimental studies verify the workings of the proposed QZSI. The derived expressions for designing the network passive components and various parameter values are listed in Table 3. The studies are presented as follows:

Table 3. Values of the parameters.

Parameters	Design Formula	Value
L_1,L_2, L_3	$L_1=\frac{(1+2D_{sh})(1-D_{sh})V_{in}}{2(1-2D_{sh})\Delta I_{L1}.F_s};L_2=\frac{D_{s7}V_{in}}{\Delta I_{L2}.F_s};L_3=\frac{D_{sh}(1-D_{sh})V_{in}}{(1-2D_{sh})\Delta I_{L3}.F_s}$	0.6 mH
C_1,C_2,C_3	$C_1=\frac{D_{s7}V_{in}}{\Delta V_{C1}.F_s};C_2=\frac{3M^2D_{s7}V_{in}}{8R(1-D_{s7})^2\Delta V_{C2}.F_s};C_3=\frac{3M^2D_{sh}V_{in}}{8R(1-2D_{sh})^2\Delta V_{C3}.F_s}$	220 µF
F_s	-	10 kHz

4.1 Simulation studies

The working of the suggested QZSI is tested under different gains of 2.5 and 3.3. The results are shown in Figure 9. The input voltage (V_{in}) is 80 V and 54 V in the two gain cases respectively. The reference peak value of output voltage (V_o) is 90 V in Figure 6. In case of gain of 2.5 (Figure 9a), the two capacitors' (V_{c2} and V_{c3}) and peak of DC-bus voltages (V_{dc}) are calculated using (4) - (6) and found as 180 V, 20 V and 200 V, respectively. In the gain of 3.3 (Figure 9b), the voltages are 180 V, 0 V and 180 V, respectively according to (8) - (10). The responses in Figure 8 agree with the calculated values.

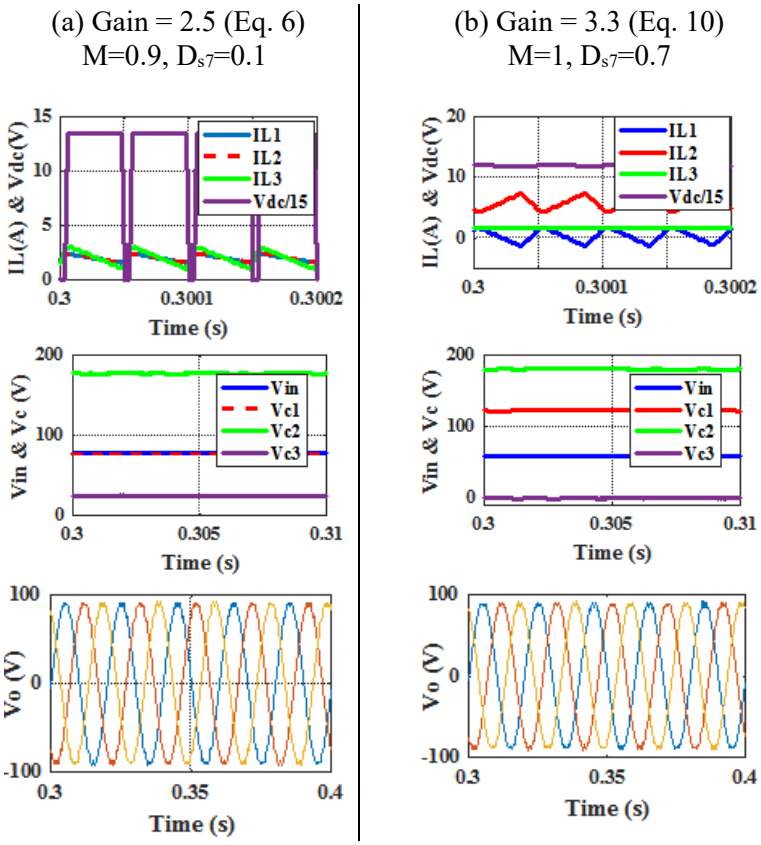

Figure 9. Various responses at two different gains.

4.2 Experimental studies

The proposed QZSI (MOSFET switch-TOSHIBA: 2sk3878) are tested in hardware as per Figure 6 with the controller (NUCLEO-G474RE Development Board) and the driver (TLP 250). The hardware set up is shown in Figure 10. Figure 11 shows the various captured responses. The performance is almost similar to that of the respective simulation study of Figure 9.

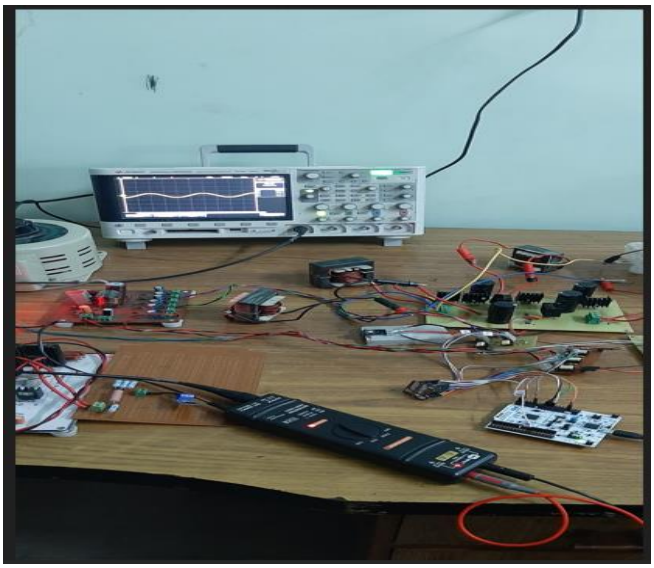

Figure 10. Proposed QZSI in Test Setup.

(a) Gain = 2.5 (Eq. 6)
M=0.9, D_{s7}=0.1

(b) Gain = 3.3 (Eq. 10)
M=1, D_{s7}=0.7

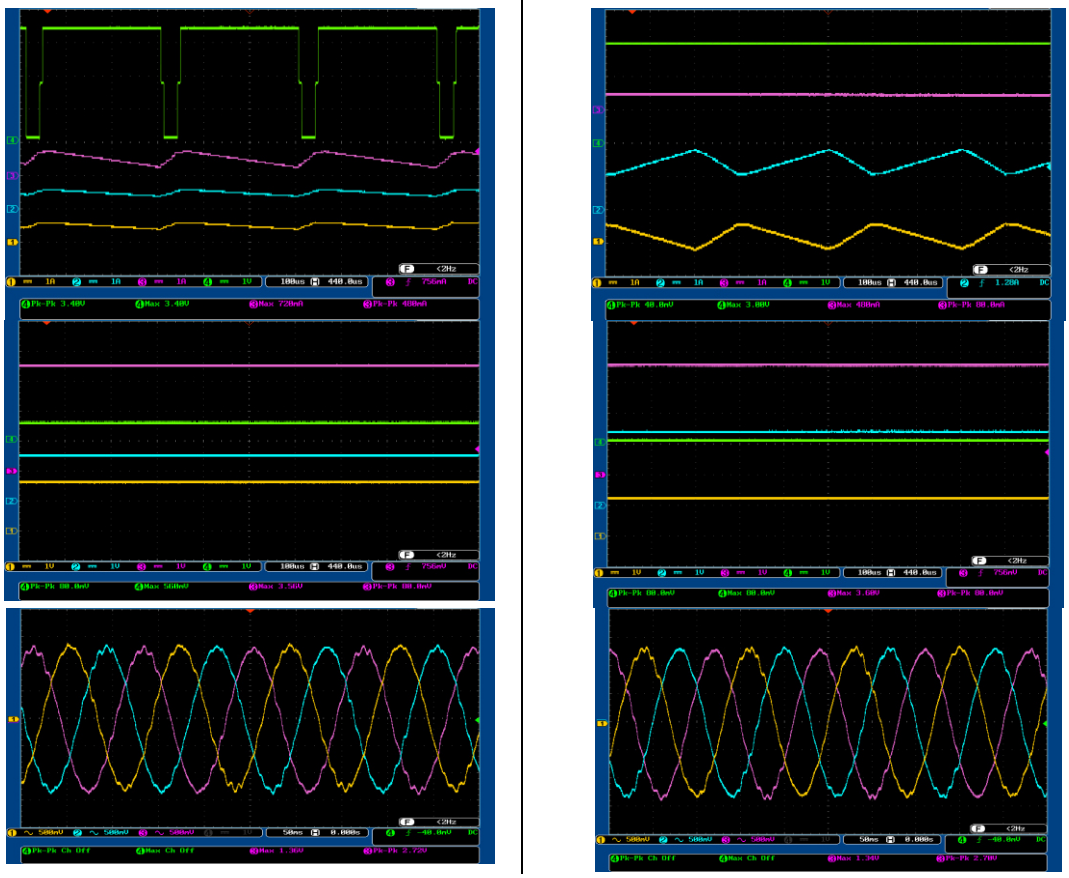

Figure 11. Experimental responses and scales: V_{dc} (1:60); V_c,V_{in} &V_o(1:50); I_L(1:4).

5 Conclusion

An improved quasi-z-source network has been introduced in this paper. The merits of the suggested inverter are mentioned as follows: (i) the DC-side voltage gain is achieved through combined duty ratio controls during shoot-through and non-shoot-through operations; (ii) enhanced voltage gain is achieved through non-shoot-through duty ratio control; (iii) the non-shoot-through duty ratio is decoupled from modulation index for getting variable DC-side voltage gain at a fixed value of modulation index; (iv) operation at M = 1 with variable voltage gains is permitted; (v) elimination of shoot-through state at higher gain operation reduces losses; (vi) in addition to control freedom, the shoot-through-prone DC-side voltage gain is augmented through the suggested active switched qZSI at low gain operation. The diverse features declare the proposed boost inverter a superior option over the existing QZSIs.

References

[1] Y. Li, J. Anderson, F. Z. Peng, and D. Liu, “Quasi-Z-source inverter for photovoltaic power generation systems,” in *Proc. 34th Annu. IEEE Appl. Power Electron. Conf. Expo*., 2009, pp. 918-924.

[2] Y. P. Siwakoti, F. Z. Peng, F. Blaabjerg, P. C. Loh, and G. E. Town, "Impedance-Source Networks for Electric Power Conversion Part I: A Topological Review," *IEEE Trans. Power Electron*., vol. 30, no. 2, pp. 699-716, Feb. 2015.

[3] F. Z. Peng, “Z-source inverter,” *IEEE Trans. Ind. Appl.*, vol. 39, no. 2, pp. 504–510, Mar./Apr. 2003.

[4] A. Ho, T. Chun, and H. Kim, “Extended Boost Active-Switched-Capacitor/Switched-Inductor Quasi-Z-Source Inverters,” *IEEE Trans. Power Electron.*, vol. 30, no. 10, pp. 5681-5690, Oct 2015.

[5] Y. W. Gu, Y. F. Chen, B. Zhang, "Enhanced-Boost Quasi-Z-Source Inverter with An Active Switched Z-Network," *IEEE Trans. Ind. Electron*., vol. 65, no. 10, pp. 8372-8381, Oct. 2018.
[6] M. K. Nguyen, T. D. Duong, Y. C. Lim, J. H. Choi, "High Voltage Gain Quasi-Switched Boost Inverters with Low Input Current Ripple," *IEEE Trans. Ind. Informat.*, vol. 15, no. 9, pp. 4857-4866, Sept. 2019.
[7] X. Zhu, B. Zhang, and D. Qiu, "A high boost active switched quasi-Z-source inverter with low input current ripple," *IEEE Trans. Ind. Informat*., vol. 15, no. 9, pp. 5341-5354, Sept.2019.
[8] A. Kumar, Y. Wang, M. Raghuram, P. Naresh, X. Pan and X. Xiong, "An Ultra High Gain Quasi Z-Source Inverter Consisting Active Switched Network," *IEEE Trans. on Circuits and Systems II: Express Briefs*, vol. 67, no. 12, pp. 3207-3211, Dec. 2020.
[9] P. K. Gayen, and S Das, "An enhanced ultra-high gain active-switched quasi Z-source inverter," *IEEE Trans. on Circuits and Systems II: Express Briefs*, vol. 69, no. 3, pp. 1517-1521, Mar. 2022.
[10] S. Yang, X. Ding, F. Zhang, F. Z. Peng, Z. Qian, "Unified Control Technique for Z-Source Inverter," *Proc. of 39th IEEE Power Electronics Specialists Conference*, June 2008, pp. 3236-3242.
[11] Y. P. Siwakoti, F. Z. Peng, F. Blaabjerg, P. C. Loh, G. E. Town and S. Yang, "Impedance-source networks for electric power conversion part II: review of control and modulation techniques," *IEEE Trans. Power Electron*., vol. 30, no. 4, pp. 1887-1906, Apr. 2015.
[12] X. Li, C. Qin, and Z. Chu, "Novel Space Vector Modulation Method for the Quasi-Z-Source Asymmetrical Three-Level Inverter," *IEEE Trans. on Circuits and Systems II: Express Briefs*, vol. 71, no. 1, pp. 281-285, Jan. 2024.
[13] P. Liu, J. Xu, Y. Yang, H. Wang, and F. Blaabjerg, ''Impact of modulation strategies on the reliability and harmonics of impedance-source inverters,'' *IEEE J. Emerg. Sel. Topics Power Electron*., vol. 8, no. 4, pp. 3968-3981, Dec. 2020.
[14] A. Ravindranath, S. Mishra, and A. Joshi, "Analysis and PWM control of switched boost inverter," *IEEE Trans. on Ind. Electron.*, vol. 60, no.12, pp. 5593-5602, Dec. 2013.
[15] G. Zarei, E. Babaei, and M. B. Banae Sharifian, "Analysis, design, and implementation of switched Z-source inverter with an extra control input," *IET Power Electron.*, vol. 16, no. 13, pp. 2178-2191, Oct. 2023.
[16] M. B. Vandishi, A. L. Eshkevari, A. Salemnia, and A. Mosallanejad, ''A new quasi-Z-source switched-boost four-switch three-phase inverter with independent shoot-through and non-shoot-through modulation indexes,'' *IET Power Electron*., vol. 14, no. 3, pp. 548-561, Jan. 2021.
[17] M. Shen and F. Z. Peng, "Operation modes and characteristics of the z-source inverter with small inductance or low power factor," *IEEE Trans. on Ind. Electron*., vol. 55, no. 1, pp. 89-96, Jan 2008.
[18] T. Kayiranga, H. Li, X. Lin, Y. Shi, and H. Li, "Abnormal operation state analysis and control of asymmetric impedance network-based quasi-z-source pv inverter (ain-qzsi)," *IEEE Trans. on Power Electron*., vol. 31, no. 11, pp. 7642-7650, Nov 2016.
[19] A. Abdelhakim, P. Davari, F. Blaabjerg, P. Mattavelli, "Analysis and Design of the Quasi-Z-Source Inverter for Wide Range of Operation", *2018 IEEE 19th Workshop on Control and Modeling for Power Electronics (COMPEL)*, pp.1-6, 2018.